Non-stationary Australasian Teleconnections

Ailie J. E. Gallant, Steven J. Phipps, David J. Karoly, A. Brett Mullan, Andrew M. Lorrey

Email: ailie.gallant@monash.edu

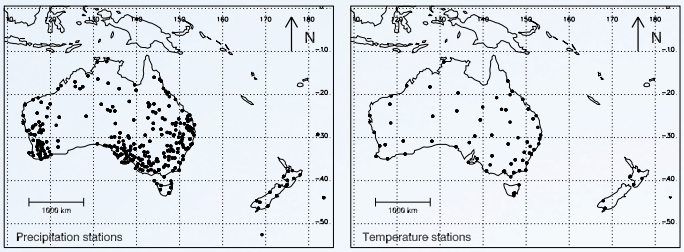

Figure 1. The Australasian domain (55°S – 0°S, 110°E –175°W) and the locations of the instrumental precipitation (left panel) and mean temperature (right panel) stations used in this study.

The assumption of stationary relationships between local and remote climates is tenuous for many seasonal relationships between interannual variations in the El Niño–Southern Oscillation (ENSO) and the Southern Annular Mode (SAM), and Australasian precipitation and mean temperatures.

Non-stationary local-remote climatic relationships were detected on near-centennial time scales from instrumental data and climate model simulations, showing they are inherent in environments regulated by internal variability.

METHOD

Statistical relationships between local and remote climates were measured as 31-year running correlations. Non-stationary relationships were defined as a change in the strength and/or phase of that correlation that was outside the range expected from stationary local climate noise.

Observed and modelled 31-year running correlations were compared to the possible range expected from a stationary teleconnection, calculated using synthetic 31-year running correlations, defined as

$$v(t) = \alpha_0 + \alpha_1 c(t) + \sigma_v \sqrt{1-r^2}\left(\eta_v(t) + \beta\eta_v(t-1)\right)$$

- $v(t)$ is the synthetic precipitation/temperature series.
- α_0, α_1 describe the regression relationship between local precipitation/temperature and SAM or ENSO, $c(t)$.
- Final term describes the magnitude of the local climate noise that influences the strength of this regression relationship.

RESULTS

The relationships between ENSO and SAM and Australasian precipitation were non-stationary at 21%–37% of Australasian stations from 1900–2009 and strongly covaried, suggesting common modulation (Figure 2).

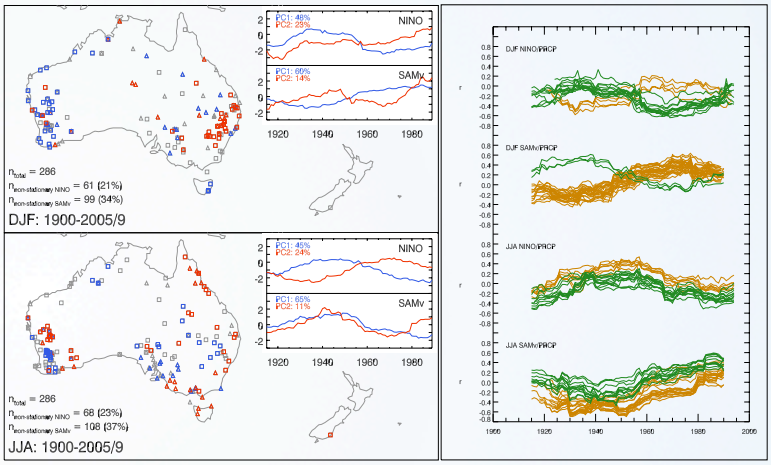

Figure 2. a) Stations where there were non-stationary relationships between precipitation and the Niño 3.4 (triangles) and Visbeck SAM (squares) indices from 1900–2005/2009 during DJF (upper panel) and JJA (lower panel). The 30% of stations most strongly loading the first (blue) and second (red) EOFs computed from the running z-scores are in color. The inset plots show the standardized variations of the principal components associated with each EOF. The variance explained by each component is provided in the top left of each plot.

b) Shows the time series from the 30% of stations most strongly loading the first EOFs of the 31-year running correlations, indicated by the labels, from 1900–2005/9. The orange time series are from stations in the western half of the domain and the green from the eastern half of the domain, defined as west or east of 130°E.

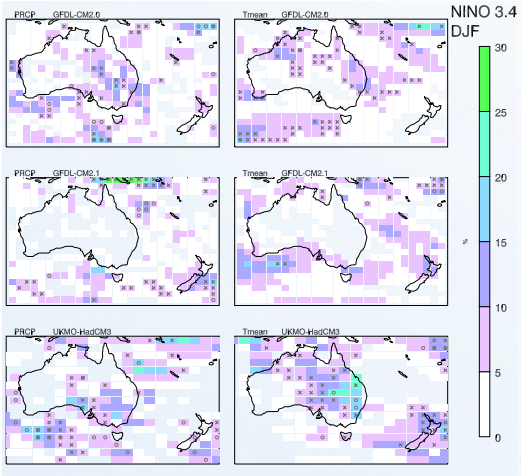

Figure 3. Shading indicates the percentage proportion of the time series for which non-stationarities were detected in the relationship between the modeled Niño 3.4 index and Australasian precipitation (left column) and temperatures (right column) during DJF. Non-stationary relationships are shown for the GFDL-CM2.0 (upper row), GFDL-CM2.1 (middle row) and UKMO-HadCM3 (lower row) simulations. Grid boxes where the timing of non-stationarities coincided with statistically significantly deviations in the 31-year mean or standard deviation of the model Niño 3.4 index are illustrated by the circles and the crosses respectively.

The non-stationarities coincided with changes in variance of the ENSO and SAM indices at over 23% of precipitation stations during JJA, and over 16% during DJF. Thus, internal changes in the ENSO and SAM often explained the observed behavior, rather than changes in the teleconnections.

Control simulations from three coupled GCMs produced ENSO-like and SAM-like patterns of variability, but differed in detail to the observed teleconnection patterns with Australasia. However, the internal teleconnections in the GCMs also displayed non-stationarities, sometimes in over 50% of the domain (Figures 3 and 4).

Gallant, A. J. E., Phipps, S. J., Karoly, D. J., Mullan, A. B. and Lorrey, A. M., 2013: Non-stationary Australasian Teleconnections and Implications for Paleoclimate Reconstructions, *Journal of Climate*, **26**, 8827-8849.

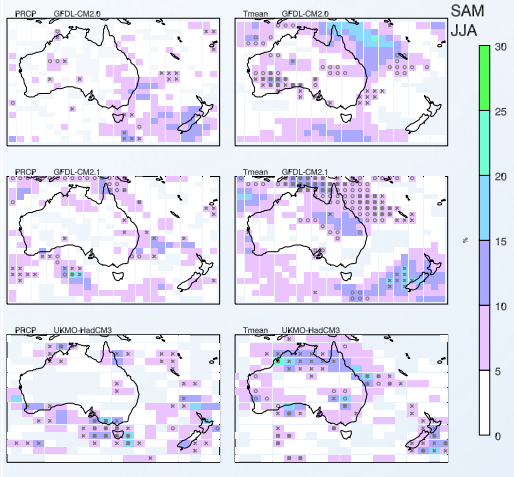

Figure 4. Shading indicates the percentage proportion of the time series for which non-stationarities were detected in the relationship between the modeled SAM index and Australasian precipitation (left column) and temperatures (right column) during JJA. Non-stationary relationships are shown for the GFDL-CM2.0 (upper row), GFDL-CM2.1 (middle row) and UKMO-HadCM3 (lower row) simulations. Grid boxes where the timing of non-stationarities coincided with statistically significantly deviations in the 31-year mean or standard deviation of the model SAM index are illustrated by the circles and the crosses respectively.